Pergamon

Int. J. Heat Mass Transfer. Vol. 39, No. 14, pp. 2915–2923, 1996

0017-9310/96 $15.00 + 0.00

0017-9310(95)00382-7

Nozzle-geometry effects in liquid jet impingement heat transfer

SURESH V. GARIMELLA and BORIS NENAYDYKH

Department of Mechanical Engineering, University of Wisconsin-Milwaukee, P.O. Box 784, Milwaukee, WI 53201, U.S.A.

(*Received* 7 *August* 1995 *and in final form* 19 *October* 1995)

Abstract—Experiments were conducted to determine the effect of nozzle geometry (diameter and aspect ratio) on the local heat transfer coefficients from a small heat source to a normally impinging, axisymmetric, submerged and confined liquid jet of FC-77. A single jet with nozzle diameters in the range of 0.79–6.35 mm and up to seven different nozzle aspect ratios in the range of 0.25–12 were tested, at turbulent jet Reynolds numbers from 4000 to 23 000 and nozzle to heat source spacings of 1–14 jet diameters. The results indicate that at very small nozzle aspect ratios ($l/d < 1$), the heat transfer coefficients are the highest. As the aspect ratio is increased to values of 1–4, the heat transfer coefficients drop sharply, but with further increases in l/d of up to 8–12, the heat transfer coefficients gradually increase. This effect is less pronounced as the nozzle to target spacing is increased. Possible explanations for these trends are provided in terms of flow separation at the nozzle entrance and its effect on the exit velocity profiles. The nozzle diameter also has a definite effect on the heat transfer coefficients. Copyright © 1996 Elsevier Science Ltd.

INTRODUCTION

Impinging jets have been actively studied for application in diverse situations such as drying, steel mills and turbine-blade cooling. Jet impingement is also being adapted for use in cooling electronic components. The increased power dissipation in chips with ever higher component-densities has necessitated the search for more effective cooling techniques. The influence of nozzle geometry on the heat transfer obtained from impinging liquid jets is investigated in this paper with jet and heat-source dimensions that are representative of electronics cooling applications.

The parameters that have been widely considered in the jet-impingement literature are nozzle diameter, nozzle to target spacing, and Reynolds number. The influence of the shape of the nozzle, contoured vs square-edged, has also been examined. Fewer studies have investigated the roles of the diameter and the length-to-diameter ratio of the nozzle on heat transfer. Although a wide variety of nozzle geometries have been studied, ranging from long tubes with fully developed outflow to knife-edged orifices, a systematic investigation of the influence of these two parameters on heat transfer has not been reported for confined and submerged liquid jets. The impingement heat transfer is affected by the nozzle aspect ratio primarily through the velocity profile and turbulence levels at the nozzle exit, which depend upon its diameter and length.

The jets considered in this study are axisymmetric and submerged, with the jet issuing into a region containing the same liquid at rest. The radial spread of the jet upon impingement is confined in a narrow channel bounded by the impingement surface and a plate containing the nozzle; this arrangement has also been referred to as semi-confined in the literature [1]. It has been shown that enhanced heat transfer is obtained in submerged configurations [2], but that, conversely, confinement causes a reduction in heat transfer; this reduction was shown to be as much as 50% for submerged air jets at small nozzle-to-target spacings [1].

An impinging jet starts being influenced by the presence of the target surface approximately 1.2 nozzle diameters from the surface [3, 4]. In this impingement region, the flow is decelerated in the axial direction and accelerated in the radial direction. The potential core of the jet strikes the impingement surface when the nozzle-to-target spacing is smaller than the length of the core, which was shown for turbulent jets to be 6–8 nozzle diameters long with well-formed nozzles, and 2–3 diameters with square-edged orifices [5]. The stagnation Nusselt number has been observed to increase slightly, or remain constant, as Z/d increases from 1 to about 4, for a wide range of Reynolds numbers [6–9]. In this Z/d range, the axial velocity of the jet remains constant explaining the relative constancy of the stagnation Nusselt number. At larger Z/d, where impingement occurs beyond the potential core, the axial velocity decreases with increasing distance and the level of turbulence begins to increase due to the large-scale structures in the mixing region. The decreasing axial velocity results in decreasing stagnation heat transfer coefficients. This trend also holds for the average Nusselt number [2].

The local heat transfer coefficient distribution in submerged liquid jet impingement has been inves-

NOMENCLATURE

A_h	heated area of heater
d	nozzle diameter
h	local convective heat transfer coefficient
$\bar{h}$	area-averaged heat transfer coefficient
h_0	stagnation point heat transfer coefficient
k	fluid thermal conductivity
l	nozzle plate thickness
Nu	local Nusselt number (hd/k)
Nu_0	stagnation Nusselt number ($h_0 d/k$)
Pr	fluid Prandtl number
q_{out}	power dissipated by the heater
r	radial distance from the stagnation point
Re	Reynolds number (Ud/ν)
T_j	jet exit temperature
T_s	heater surface temperature
U	mean velocity of the jet
Z	distance between the confining plates.

Greek symbols

ρ	fluid density
ν	fluid kinematic viscosity.

Subscript

f	parameters with properties based on film temperature.

tigated in several studies [6–12]; of these, only a few [6, 10–12] have considered a submerged impingement flow field that was confined by a top wall. Local heat transfer distributions for (submerged) air jets are reported in [3, 13–16]. The local heat transfer coefficient on the impingement surface has been found to have a bell-shaped distribution with respect to radial distance from the stagnation point. The maximum value occurs near stagnation and decreases symmetrically with radial distance. In addition to the peak at stagnation, secondary maxima have been observed in the local heat transfer coefficient curves near $r/d \approx 2$. Transition to turbulence was established as a likely cause for the secondary peak, which disappeared with increasing Z/d, and decreasing jet Reynolds number ($Re < 2500$). At very small Z/d (as low as 0.1–0.25), a second set of secondary peaks has been observed for confined and unconfined air jets in the vicinity of $r/d \approx 0.5$, and was attributed to accelerated radial flow [17, 18].

A number of studies have investigated the role of nozzle shape on exit velocity profiles and impingement heat transfer. Popiel and Boguslawski [19] compared the performance of a contoured nozzle to a sharp-edged orifice. Mass-transfer rates for the orifice were as much as 40% higher than those for the contoured nozzle due to increased turbulence levels from the orifice. The increased turbulence also appeared to limit the development of ordered structures in the jet mixing layer. The potential core for the orifice was significantly shorter than for the contoured nozzle. Stevens *et al.* [20] showed with velocimetry measurements in free-surface liquid jets that the turbulence level in jets from sharp-edged orifices was higher than from contoured nozzles; Pan *et al.* [21] showed in a companion paper that the resulting differences in the heat transfer coefficients were on the order of 40%. In otherwise similar experiments with converging [22] and rectangular [23] slot jets of water, the converging nozzles had more uniform velocity profiles and hence significantly lower heat transfer coefficients than for rectangular nozzles, due to the higher centerline velocities present in the latter, when the two were run at identical average velocities.

Fewer studies have considered the influence of nozzle geometry (diameter and aspect ratio) on the heat transfer from an impinging jet. Obot *et al.* [24] presented a detailed study of the effect of nozzle aspect ratio for submerged (but unconfined) air jets. Experimental results were obtained for nozzles with 5 l/d's in the range of 1–50, at a constant diameter. Womac *et al.* [2] used orifices ranging in diameter from 0.978 to 6.55 mm (aspect ratios from 18.4 to 2.74) and found markedly different average Nusselt numbers for a given Reynolds number and Z/d. Mohanty and Tawfek [16] found significantly different heat transfer distributions for their tapered nozzles ranging in diameter from 3 to 7 mm (aspect ratio not stated). In contrast, Hollworth and Gero [15] obtained identical local Nusselt numbers for square-edged nozzles 5 and 10 mm in diameter with an aspect ratio (l/d) of 1, when tested at the same Reynolds number and Z/d. For free-surface liquid jets [25, 26] it was found that the stagnation Nusselt number characteristics were dependent on nozzle diameter. This was attributed to the influence of free-stream velocity gradient on local heat transfer, and different correlations were proposed for each of the four nozzle diameters (from 2.2 to 8.9 mm) studied. The length of the nozzle is also an important parameter: the more uniform exit velocity profiles in shorter nozzles result in lower heat transfer coefficients than for longer nozzles with fully developed exit profiles [27, 28].

The present study experimentally investigates the influence of nozzle geometry, specifically the nozzle diameter and the length-to-diameter aspect ratio, of a square-edged nozzle on the local heat transfer distribution on a small heat source, in *submerged* and

confined liquid jet impingement. Besides the nozzle geometry (d and l/d), the experimental variables include jet Reynolds number (Ud/ν) and nozzle-to-target spacing (Z/d).

EXPERIMENTS

The experiments were conducted in a transparent, closed-loop liquid jet impingement facility which is the same as that described in [6, 12, 29], and only important details are included here. The technique for obtaining local heat transfer measurements was to hold the jet stationary while moving the heat source. The heat source is an electrically heated foil with a thermocouple attached to the underside. Since lateral conduction along the very thin foil can be neglected ($< 0.5\%$ of heat flow perpendicular to the foil) and all the heat is lost by convection to the jet, the thermocouple reads a local temperature; as the heat source translates laterally, the heat transfer distribution on the heat source is mapped.

The coolant used in the experiments is a perfluorinated dielectric liquid, FC-77, which has a Prandtl number of 25.3 at the nozzle exit temperature which is maintained constant at 20°C. The test section is made of plexiglass and houses a flow-conditioning plenum with a nozzle plate attached to one end. Facing the nozzle plate is a target plate containing the heat source, as shown in Fig. 1. A T-type thermocouple near the base of the plenum measures the fluid temperature just prior to its exit from the nozzle. Since the cross-sectional area of the plenum is larger than that of the largest nozzle used in this study by a factor of 196, the velocity inside the plenum can be considered negligible compared to the jet velocity (with low upstream turbulence). A number of nozzle plates (one plate for each nozzle geometry) were used in the experiments. Each plate is 12.7 cm in diameter with thickness (nozzle length, l) ranging from 0.79 to 38.1 mm, and has a square-edged nozzle in the center.

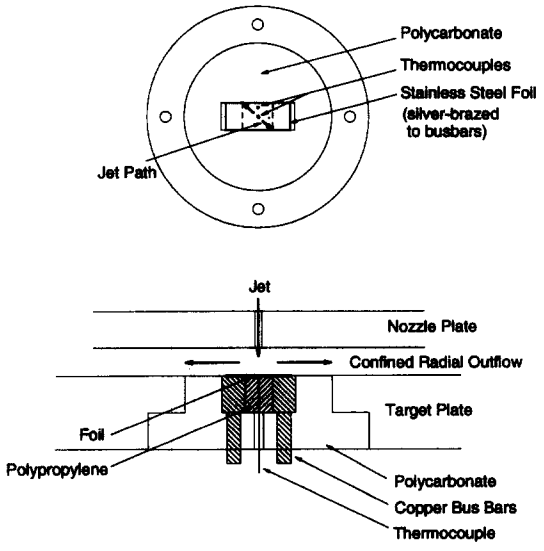

Fig. 1. Schematic of the submerged and confined liquid jet impingement setup and heat source assembly; "Jet Path" indicates the direction of horizontal traversal of the heat source relative to the stationary jet.

The plenum assembly is designed to translate in the vertical direction in increments of 0.01 mm so that the nozzle-to-target spacing (Z/d) can be accurately set. Fluid from the nozzle impinges on the heater mounted in the target plate (Fig. 1). The heater was made by silver brazing the ends of a 0.075 mm thick stainless steel foil to copper bus bars; the resulting square heat source is 10 mm on the side. Care was taken to ensure that the braze joint was uniform and continuous across the width of the bus bars. The resistance heating in the foil thus begins precisely at the edge of the bus bar. The joint location was verified by inspecting the joint visually and comparing the measured resistance of the heater to theoretical values. The very small thickness of the foil minimizes heat conduction in the lateral direction, allowing for the measurement of a local surface temperature. As the heat source is moved laterally with respect to the jet, local surface temperatures are obtained; this mimics an arrangement with a large number of thermocouples under a stationary heat source.

The foil heater is backed by insulation with through-holes to accommodate two 36 gage T-type thermocouple leads. One thermocouple is at the center of the heater and the other is 3 mm from the center (see Fig. 1), the beads of each being flush with the surface of the insulation. The insulating polypropylene block is attached to the foil using a high-temperature adhesive transfer tape across which the temperature drop can be accurately calculated, a typical value being about 0.1°C. The foil-backing assembly fits snugly into a circular polycarbonate holder for structural integrity which is in turn inserted into a larger target plate. The target plate can be traversed horizontally in fine increments relative to the jet. The heater is oriented in the target plate such that the center of the jet traverses diagonally across the heater, such that measurements are made at the farthest edges of the heated surface. The thermal boundary condition on the impingement surface was thus that of a constant heat flux over the square heat source, surrounded by an insulating target plate. Since the extent of traversal of the jet on the heat source is limited to the heated area (no unheated starting length), the thermal boundary layer development is not altered as the heat source is moved relative to the jet.

The current in the circuit is determined by measuring the voltage drop across a 100 A current shunt; the voltage drop across the foil heater is measured across the base of the copper bus bars. The product of the current and the voltage drop across the heater gives the power dissipated (q_{out}). As described in Garimella and Rice [6], all the power dissipation occurs in the 100 mm^2 patch of heater foil between the bus bars, due to the negligible contact resistance in the

voltage-drop measurement. A conduction analysis (using measured temperatures at the top and bottom of the polycarbonate insert) showed that the heat lost through the polypropylene block on the underside of the foil was less than 2%; this loss was calculated as part of the data acquisition program and subtracted from the total heat dissipation. The local heat transfer coefficient was calculated as:

$$h = \frac{q_{\text{out}} - q_{\text{loss}}}{A_{\text{h}}(T_{\text{s}} - T_{\text{j}})} \tag{1}$$

where the heat flux and T_{j} are constant in an experiment, while T_{s} depends on location on the heat source. The data from each experiment were also area-averaged (over the area of the square heat source) to obtain an average heat transfer coefficient:

$$\bar{h} = \frac{q_{\text{out}}}{\Sigma[(T_{\text{s}_i} - T_{\text{j}})A_i]} \tag{2}$$

where T_{s_i} is the local surface temperature measured for the area A_i of the annular band straddling the location of each temperature measurement; at the corners of the square heat source, the annuli are fragmented. The summation in the denominator of equation (2) is performed over the area of the heater, A_{h}. Typical values for $(T_{\text{s}} - T_{\text{j}})$ were in the range of 10–30°C for a heat flux of 25 W cm^{-2}. Each temperature was calculated as an average of 50 thermocouple readings. The heat flux was adjusted in the experiments to maintain relatively constant (surface-average) temperature differences between the heat source and jet. The thermophysical properties in the nondimensional parameters (Nu, Re and Pr) were all evaluated at the jet inlet temperature, except for the correlations [equations (3) and (4)], which are evaluated at the film temperature.

A standard uncertainty analysis indicated that the uncertainty in the heat transfer coefficient was on the order of 5% (20:1 odds) in all cases. The primary contribution ($\approx$4%) to the uncertainty comes from the heater-area measurement; uncertainty in temperature measurement is the other significant contributor. The uncertainties in the voltage and current were taken as twice the standard deviation of the measured values. The uncertainty in each temperature measurement was taken to be 0.3°C, and the uncertainty in the heat-source area was estimated at 4%. Experiments performed over a period of more than a year were found to have excellent repeatability, with the spread never greater than 3%; the heat transfer coefficient curves were also highly symmetric about the heater centerline.

Four jet diameters of 0.79, 1.59, 3.18 and 6.35 mm, each with up to seven aspect ratios in the range $0.25 \leqslant l/d \leqslant 12$, were studied for jet Reynolds numbers ranging from 4000 to 23 000, nozzle-to-target spacings (Z/d) from 1 to 14, and a large number of radial positions in $0 \leqslant r \leqslant 7$ mm ($r/d \leqslant 8.9$ for $d = 0.79$ mm, to $r/d \leqslant 1.11$ for $d = 6.35$ mm).

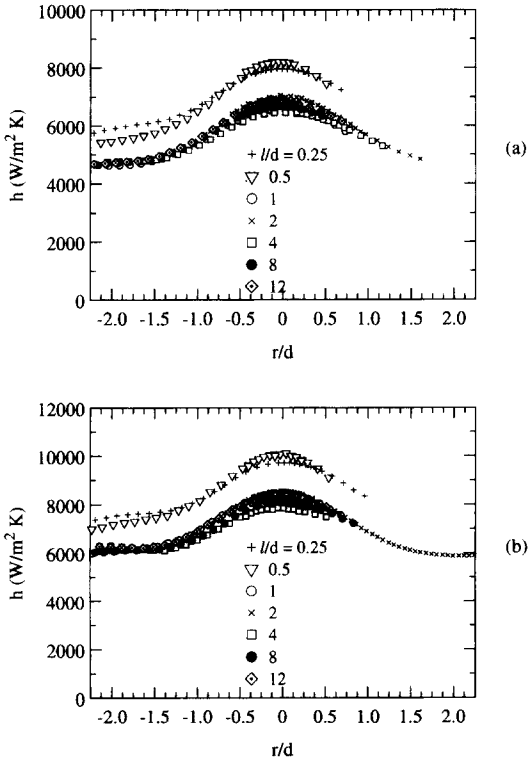

Fig. 2. Variation in local heat transfer coefficient distribution with nozzle aspect ratio for a nozzle diameter of 3.18 mm and $Z/d = 4$ for (a) $Re = 8500$ and (b) $Re = 13\,000$.

RESULTS AND DISCUSSION

The distribution of the heat transfer coefficient on the heat source is illustrated as a function of radial distance from the stagnation point for a nozzle diameter of 3.18 mm, a spacing of $Z/d = 4$, and two Reynolds numbers of 8500 and 13 000, in Fig. 2. The nozzle aspect ratio (l/d) is varied in these graphs from 0.25 to 12. The heater extends over 2.25 nozzle diameters for this nozzle. The curves in Fig. 2 are bell-shaped, with a peak at the stagnation point. The heat transfer coefficient decreases as radial distance from the stagnation point increases. It is clear from the curves at both Reynolds numbers that the very short ("knife-edged") nozzles with aspect ratios of 0.25 and 0.5 yield heat transfer coefficients that lie well above all the other curves. Moreover, the heat transfer coefficients (at any r/d) drop as the aspect ratio increases to an l/d of 1–4, and then recover somewhat (increase in value) for further increases to an l/d of 8–12. The change in heat transfer with aspect ratio is most distinct, however, between the ranges $l/d < 1$ and $l/d \geqslant 1$. These trends are observed at both Reynolds numbers in Fig. 2, and were true for all Reynolds numbers tested in this study.

Figure 3 shows heat transfer distributions with the same nozzle as in Fig. 2, for $Re = 8500$ but at smaller and larger nozzle to target spacings of $Z/d = 2$ and 8. As in Fig. 2, the heat transfer initially decreases with increasing nozzle aspect ratio. For increases of l/d

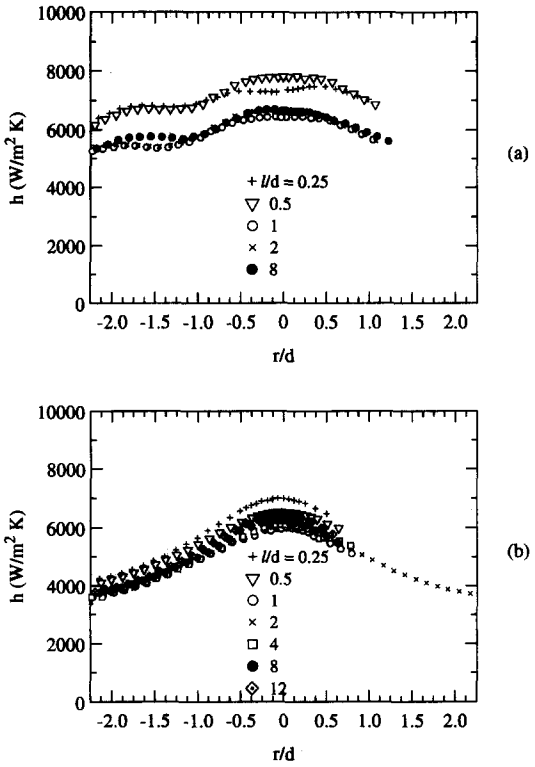

Fig. 3. Variation in local heat transfer coefficient distribution with nozzle aspect ratio from a nozzle diameter of 3.18 mm and $Re = 8500$ for (a) $Z/d = 2$ and (b) $Z/d = 8$.

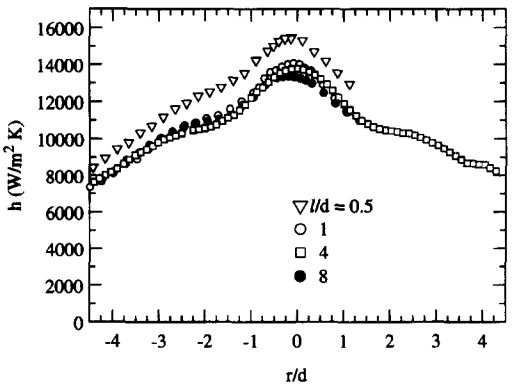

Fig. 4. Variation in local heat transfer coefficient distribution with nozzle aspect ratio for a nozzle diameter of 1.59 mm, $Z/d = 4$ and $Re = 13\,000$.

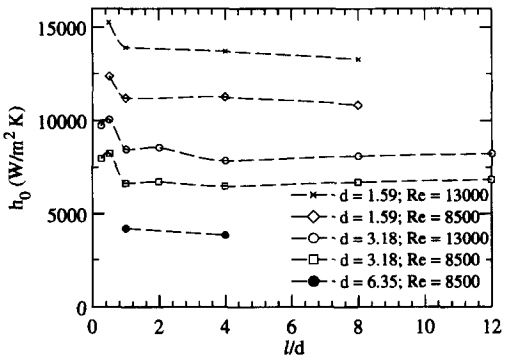

Fig. 5. Effect of nozzle aspect ratio on the stagnation heat transfer coefficients for different jet diameters (mm) and Reynolds numbers at a spacing of $Z/d = 4$.

beyond 1, however, the heat transfer coefficients increase again, at both spacings. This minimum in heat transfer with nozzle aspect ratio occurs at $l/d = 4$ for $Z/d = 4$ (Fig. 2) and at $l/d = 1$ for $Z/d = 2$ and 8 (Fig. 3). The other difference between the behavior at the different spacings is the extent of the influence of aspect ratio on heat transfer: the spread with l/d in the area-averaged heat transfer coefficients at $Z/d = 2$ and 4 was 20%, whereas this spread at $Z/d = 8$ was reduced to 14%. It may thus be concluded that the nozzle aspect ratio plays a more dominant role in determining heat transfer coefficients at the smaller nozzle spacings. In contrast to Z/d, the role of aspect ratio on heat transfer is unaffected by the Reynolds number in question. This would be expected for heat transfer near the stagnation region since at the smaller spacings, the pre-impingement potential core of the jet is largely inviscid, and the Reynolds number would not be a relevant governing parameter. These trends, shown in Figs. 2 and 3 for $d = 3.18$ mm, were also found to hold for the other three diameters studied. Figure 4 presents results for $d = 1.59$ mm at $Z/d = 4$ and $Re = 13\,000$; the curve for the smallest aspect ratio of 0.5 lies well above those for l/d of 1–8, which lie in a nearly identical group.

The stagnation point heat transfer coefficient for several different nozzle diameters and Reynolds numbers is plotted as a function of nozzle aspect ratio in Fig. 5 for a fixed nozzle to target spacing of $Z/d = 4$.

The corresponding average heat transfer coefficients are shown in Fig. 6. It should be recalled that the area-averaged results presented here were averaged over the (fixed) actual area of the heat source, and thus, not over the same r/d for all nozzle diameters. These figures clearly demonstrate the effect of nozzle aspect ratio on both the stagnation and the average heat transfer coefficients. At $l/d < 1$, both stagnation and average heat transfer coefficients are significantly

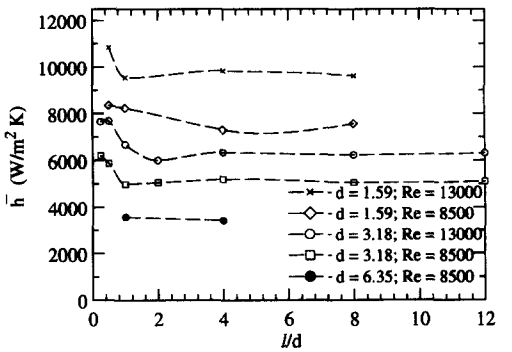

Fig. 6. Effect of nozzle aspect ratio on the area-averaged heat transfer coefficients for different jet diameters (mm) and Reynolds numbers at a spacing of $Z/d = 4$.

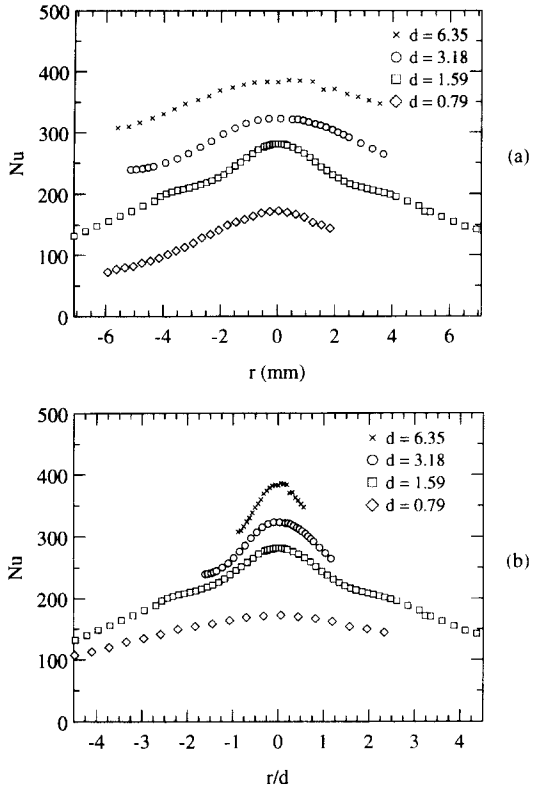

Fig. 7. Local Nusselt numbers for nozzles of different diameters (mm) with $l/d = 4$, $Z/d = 4$ and $Re = 8500$, as a function of (a) radius and (b) nondimensional radius, r/d.

higher than for $l/d \geqslant 1$; in this latter range, the influence of aspect ratio is less pronounced.

With the local heat transfer coefficients (nondimensionalized as Nusselt numbers, hd/k) plotted as a function of radius for different nozzle diameters but at a fixed l/d as in Fig. 7(a), it becomes clear that the data for each nozzle diameter lie distinct from the others for a given Re, l/d and Z/d. Although results for different diameters were not presented in their paper, Hollworth and Gero [15] observed from experiments with geometrically similar nozzles of different diameters that the local Nusselt number distribution was independent of d for a given Z/d and Re; this result is in contrast to the present observations. Garimella and Rice [6] also found a dependence on diameter, but since their nozzles were not all of the same aspect ratio (not geometrically similar), they allowed the possibility that this could be due, at least in part, to an underlying dependence on nozzle aspect ratio. Since the curves in Fig. 7(a) for different diameters are *at the same nozzle aspect ratio*, and still do not collapse, this points to a definite dependence of heat transfer on nozzle diameter. Stevens and Webb [25] also found such a dependence for free-surface liquid jets.

While an unequivocal explanation for this dependence cannot be advanced at this stage, there is evidence in the literature to suggest that the turbulence intensity near the jet centerline is larger for larger-diameter nozzles, with all other parameters (Re, l/d, Z/d) held constant. Kataoka *et al.* [30] found in experiments with submerged jets of water that the centerline turbulence intensity for a 28 mm-diameter jet was larger than that for a 14 mm-diameter jet, by amounts ranging from roughly 50% at an axial distance of two diameters from the jet exit, to 13% at a distance of six diameters at a Reynolds number of 10 000. The jet exit had a uniform velocity distribution with low initial turbulence (< 2%); the source for turbulence generation in the jet was shown to be large-scale eddies, visualized with hydrogen bubbles. This trend is consistent with the observed dependence of Nusselt numbers on diameter in Fig. 7: the larger Nusselt numbers obtained for the larger-diameter nozzles may reflect larger turbulence intensities. The jet turbulence intensity may thus be yet another parameter (independent, and not adequately characterized by Reynolds number alone) that must be taken into account when comparing jet impingement heat transfer rates.

One other point of note about Fig. 7(a) is that the radius range of roughly seven diameters included on the abscissa represents the diagonal distance of travel across the heater surface. It is instructive to consider, instead, a nondimensional abscissa in terms of r/d as shown in Fig. 7(b). Figure 7(b) could be considered to be from a point of reference attached to the jet, while Fig. 7(a) is with respect to the heat source. The curves that are well-separated in Fig. 7(a) over the entire extent of the heater reveal different information in Fig. 7(b). It appears that the differences in heat transfer between nozzles of different diameter are most pronounced close to stagnation, over an area of about one jet diameter. Beyond this region, the diameter effect on the Nusselt number distribution appears to diminish (especially for the three larger nozzle diameters). This observation holds for all the nozzles over the full range of Reynolds numbers tested, as shown in Fig. 8 for $Re = 13\,000$.

The observed influence of nozzle aspect ratio on the heat transfer distribution may be explained as follows.

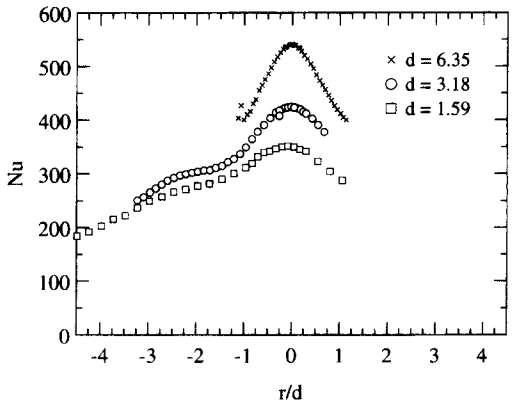

Fig. 8. Local Nusselt numbers for nozzles of different diameters (mm) with $l/d = 1$, $Z/d = 4$, and $Re = 13\,000$, as a function of nondimensional radius, r/d.

It appears that there are three ranges of aspect ratio over which the flow through the nozzle, and the nozzle exit profile, vary.

$l/d < 1$

When liquid from the relatively quiescent plenum enters the nozzle, a separation bubble is formed at the nozzle inlet. While there is rather scant information in the literature concerning the length of the separation region at an abrupt and drastic reduction in diameter, there is fairly consistent evidence that this separation bubble is just under one diameter in (streamwise) length. For instance, McGuinness [31] showed using an oil-film visualization technique that the reattachment length for a plain (square-edged) inlet was 0.9 diameters, while that for an orifice-plate inlet was $1.9d$. Sutton *et al.* [32] reported similar values for the reattachment length. Calculations using the commercial software package, FLUENT, showed that the separation region is roughly $0.8d$ long [33], which is identical to the recommendation of Ward-Smith [34] based on flow visualization. Further, the length of the separation bubble appears to be independent of the Reynolds number in turbulent flow (for $Re > 4000$ [34]). For nozzle aspect ratios in the range $l/d < 1$, therefore, the separation region would not have reattached within the nozzle. The diameter of the nozzle is partially "obscured" by the existence of the separation bubble, affecting the exit velocity profile markedly. The outflow could thus be considered to issue from a nozzle of reduced diameter (the *vena contracta*), and thus at a higher velocity (for a constant Reynolds number); the flow area, at its narrowest, is reduced to approximately 60% of the actual nozzle cross-section [34]. Since a reduction in nozzle diameter (for the same average velocity) has been shown to cause an increase in heat transfer coefficient, this partial obstruction of the nozzle by the separation region would be expected to result in higher stagnation-region heat transfer coefficients relative to the situation when the full nozzle area is active. This is consistent with the significantly higher heat transfer coefficients observed in the preceding figures at the very small aspect ratios.

$1 \leqslant l/d \leqslant 4$

As the aspect ratio is increased past a value of 1, the separated flow at the nozzle entrance reattaches within the nozzle, and the exit velocity profile becomes nearly uniform. Since the exit flow is now distributed uniformly and over a larger area compared to $l/d < 1$, the heat transfer coefficient would be expected to be lower, as observed in the results of this study. A uniform velocity profile has been observed in the literature to result in lower heat transfer coefficients relative to fully developed profiles ([27, 28] and a comparison of the results of [22, 23]).

$l/d \geqslant 4$

As the aspect ratio is increased further, the flow in the nozzle downstream of the separation bubble has a chance to develop, and the exit velocity increasingly takes on a fully developed profile. Since all the Reynolds numbers considered in this study are turbulent, fully developed velocity conditions are attained over a relatively short distance compared to laminar flow. The fully developed velocity profile is characterized by a significantly higher velocity at the axis of the nozzle than the average; this could explain the observed gradual increase in heat transfer as the aspect ratio is increased beyond 4. The exit centerline turbulence intensities also increase as l/d increases from 1 to 10 [24].

The observation that the influence of aspect ratio on heat transfer is moderated at the higher nozzle to target spacings [comparing the results for $Z/d = 2$, 4 and 8 in Figs. 2(a) and 3] is also consistent with this explanation. As the nozzle to target spacing increases, the jet travels farther before impinging on the target. The velocity profile in the jet is influenced to a greater extent by the growing mixing layer and entrainment. The marked distinctions between the exit velocity profiles at different aspect ratios and their observed influence on heat transfer at small Z/d is thus felt to a smaller extent at the larger Z/d. Obot *et al.* [24] observed for unconfined air jets that the flow characteristics and heat transfer were independent of nozzle shape and aspect ratio for $Z/d \geqslant 12$ and also for $l/d \geqslant 10$. Finally, since all the Reynolds numbers are in the turbulent regime, and the extent of the separation bubble in the nozzle is essentially unaffected by Reynolds number [34], the Reynolds-number independence of the heat transfer variations with aspect ratio is also consistent with this explanation [as in Figs. 2(a) and (b)].

Separate correlations are proposed for the stagnation Nusselt number in the ranges $1 \leqslant Z/d \leqslant 5$ and $6 \leqslant Z/d \leqslant 14$, in view of the distinct trends noted in these regions: it was previously shown [6] that the stagnation point heat transfer coefficient (h_0) is almost independent of Z/d for $Z/d < 5$. For $Z/d > 5$, h_0 decreased with increasing Z/d. This trend is also well-documented in the literature [8, 9], and results from whether or not the potential core strikes the surface. At the larger diameters, h_0 increased slightly with Z/d at small Z/d, as has also been reported in [3,13]. The initial increase in h_0 with Z/d for the two larger nozzles may be due to increasing levels of turbulence along the center line of the jet as the end of the potential core is encountered [3].

In the correlations, the Prandtl-number exponent was held constant at 0.4 as suggested in [2, 35, 36]. The independent variables in the correlations were Reynolds number, nozzle to target spacing (Z/d) and nozzle aspect ratio (l/d), for each of which a reasonable range was considered in the experiments. Although the nozzle diameter was identified as an independent parameter affecting heat transfer in this and previous studies, it was not explicitly included in the correlations, other than for nondimensionalization. The physical mechanisms for the observed

dependence of heat transfer on nozzle diameter must be better understood (and perhaps, the jet turbulence intensities measured, as in an ongoing study by the authors) before it can be properly incorporated as a parameter in correlations. All the properties in the following correlations were evaluated at the film temperature:

$$Nu_{0_f} = 0.492\, Re_f^{0.585}\, Pr_f^{0.4} \left(\frac{Z}{d}\right)^{0.024} \left(\frac{l}{d}\right)^{-0.09}$$

$$\text{for } 1 \leqslant Z/d \leqslant 5 \quad (3)$$

$$Nu_{0_f} = 0.513\, Re_f^{0.694}\, Pr_f^{0.4} \left(\frac{Z}{d}\right)^{-0.56} \left(\frac{l}{d}\right)^{-0.04}$$

$$\text{for } 6 \leqslant Z/d \leqslant 14. \quad (4)$$

Both correlations are valid for the parameter ranges of $1.59 \leqslant d \leqslant 6.35$ mm, $4000 \leqslant Re \leqslant 23\,000$, and $0.25 \leqslant l/d \leqslant 12$. The data for the smallest nozzle diameter ($d = 0.79$ mm) showed somewhat different trends of variation with the parameters, and were not included in the correlations. The composite correlations for the three nozzles collect the data to within $\pm 10\%$.

Figure 9 shows a comparison of the present results for stagnation Nusselt number with studies in the literature at nozzle-to-target spacings of $Z/d = 2$ and 7. Results in the figure from Chang *et al.* [10] are for a submerged and confined jet ($d = 4$ mm) of R-113 for $1 \leqslant Z/d \leqslant 4$; Ma *et al.* [8] and Sun *et al.* [9] for submerged and unconfined jets ($d \approx 1$ mm) of R-113, oil and ethylene glycol; and Stevens and Webb [25] for a free-surface unconfined jet of water ($d = 2.2$ mm, the smallest used in their study). A potential-core length of five diameters was used in the calculation of Nu_0 from the correlation of Ma *et al.* [8] for $Z/d = 7$; also l/d for the present results was chosen to be 4. It appears from the figure that at the smaller Z/d the present correlation (for $1.59 \leqslant d \leqslant 6.35$ mm) agrees well with the predictions of Ma *et al.* and Sun *et al.* This confirms the observation of Obot *et al.* [1] that confinement has little effect on heat transfer at the stagnation point. The results of Chang *et al.* lie somewhat above this group, possibly due to the larger nozzle diameter used. The free-surface data of Stevens and Webb lie below all the submerged-jet data. Similar trends were obtained for $Z/d = 4$ (not shown). This is consistent with the observations in the literature that enhanced heat transfer is obtained in submerged configurations [2], relative to free-surface jets. At the larger spacing of $Z/d = 7$, a stronger Reynolds-number dependence is indicated from the present results than in Ma *et al.* The free-surface results again lie below those for the submerged jets. Comparisons are not presented for the average Nusselt number, since the size and shape of the heat source (used in the area-averaging) is different in different studies; correlations for submerged and confined liquid jets with a configuration similar to that considered here are not available in the literature.

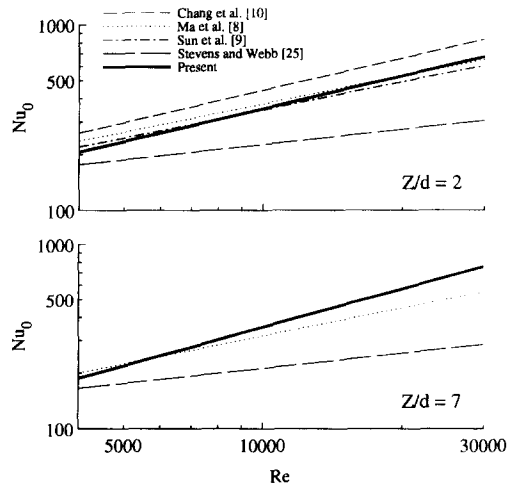

Fig. 9. Comparison of the proposed correlations for the stagnation Nusselt number [equations (3) and (4)] with studies in the literature.

CONCLUSIONS

The influence of nozzle geometry on the local heat transfer coefficient distribution on a small, square heat source was investigated in this study for submerged and confined liquid jet impingement. The nozzle (length-to-diameter) aspect ratio and diameter were explored as variables at different nozzle-to-heat source spacings and jet Reynolds numbers.

At very small nozzle aspect ratios ($l/d < 1$), the heat transfer coefficients are the highest. As the aspect ratio is increased to values of 1–4, the heat transfer coefficients drop sharply, but with further increases in l/d of up to 8–12, the heat transfer coefficients gradually increase. A possible explanation for these trends is provided in terms of flow separation and reattachment in the nozzle, and its effect on exit velocity profiles. The effect of nozzle aspect ratio is less pronounced as the nozzle to target spacing is increased. The jet Reynolds number does not appear to influence the role of nozzle aspect ratio on heat transfer.

The nozzle diameter has a definite effect on the heat transfer coefficients obtained: for fixed Reynolds number, l/d and Z/d, the local Nusselt numbers for different nozzle diameters are distinct. The differences in local Nusselt numbers obtained with different nozzle diameters are most pronounced over a region of about one nozzle diameter around the stagnation point. It is possible that this dependence of the Nusselt number on diameter is due to the increase in turbulence intensity as the nozzle diameter is increased, for a fixed Reynolds number. Correlations for the stagnation-point Nusselt number are proposed in terms of jet Reynolds number, fluid Prandtl number, nozzle to heat source spacing, and nozzle aspect ratio.

Acknowledgements—The authors wish to express their appreciation to Cray Research, Inc. of Chippewa Falls, Wisconsin, for their support of this project.

REFERENCES

1. N. T. Obot, W. J. M. Douglas and A. S. Mujumdar, Effect of semi-confinement on impingement heat transfer, *Proceedings of the Seventh International Heat Transfer Conference*, Vol. 3, pp. 395–400 (1982).
2. D. J. Womac, S. Ramadhyani and F. P. Incropera, Correlating equations for impingement cooling of small heat sources with single circular liquid jets, *J. Heat Transfer* **115,** 106–115 (1993).
3. R. Gardon and J. C. Akfirat, The role of turbulence in determining the heat transfer characteristics of impinging jets, *Int. J. Heat Mass Transfer* **8,** 1261–1272 (1965).
4. H. Martin, Heat and mass transfer between impinging gas jets and solid surfaces, *Adv. Heat Transfer* **13,** 1–60 (1977).
5. B. R. Hollworth and S. I. Wilson, Entrainment effects on impingement heat transfer—I. Measurements of heated jet velocity and temperature distributions and recovery temperatures on target surface, *J. Heat Transfer* **106,** 797–803 (1984).
6. S. V. Garimella and R. A. Rice, Heat transfer in submerged and confined jet impingement, *Heat Transfer in High Heat Flux Systems*, ASME HTD-301, pp. 59–68 (1994).
7. C. F. Ma and A. E. Bergles, Convective heat transfer on a small vertical heated surface to an impinging circular liquid jet. In *Heat Transfer Science and Technology* (Edited by B. X. Wang), pp. 193–200. Hemisphere, Washington, D.C. (1990).
8. C. F. Ma, H. Sun, H. Auracher and T. Gomi, Local convective heat transfer from vertical heated surfaces to impinging circular jets, *Proceedings of the Ninth International Heat Transfer Conference*, Hemisphere, Washington, D.C., Vol. 2, pp. 441–446 (1990).
9. H. Sun, C. F. Ma and W. Nakayama, Local characteristics of convective heat transfer from simulated microelectronic chips to impinging submerged round water jets, *J. Electron. Packaging* **115,** 71–77 (1993).
10. C. T. Chang, G. Kocamustafaogullari, F. Landis and S. Downing, Single and multiple liquid jet-impingement heat transfer, *Proceedings of ASME National Heat Transfer Conference*, Atlanta, Georgia, HTD-246, pp. 43–52 (1993).
11. G. K. Morris, S. V. Garimella and R. S. Amano, Prediction of jet impingement heat transfer using a hybrid wall treatment with different turbulent Prandtl number functions. In *Heat Transfer in Turbulent Flows*, ASME HTD-Vol. 318, pp. 1–10 (1995).
12. S. V. Garimella and R. A. Rice, Confined and submerged liquid jet impingement heat transfer, *J. Heat Transfer* **117,** 871–877 (1995).
13. J. W. Baughn, A. E. Hechanova and X. Yan, An experimental study of entrainment effects on the heat transfer from a flat surface to a heated circular impinging jet, *J. Heat Transfer* **3,** 143–149 (1991).
14. R. J. Goldstein, A. I. Behbahani and K. Kieger Heppelmann, Streamwise distribution of the recovery factor and the local heat transfer coefficient to an impinging circular air jet, *Int. J. Heat Mass Transfer* **29,** 1227–1235 (1986).
15. B. R. Hollworth and L. R. Gero, Entrainment effects on impingement heat transfer—II. Local heat transfer measurements, *J. Heat Transfer* **107,** 910–915 (1985).
16. A. K. Mohanty and A. A. Tawfek, Heat transfer due to a round jet impinging normal to a flat surface, *Int. J. Heat Mass Transfer* **36,** 1639–1647 (1993).
17. A. M. Huber and R. Viskanta, Convective heat transfer to a confined impinging array of air jets with spent air exits, *J. Heat Transfer* **116,** 570–576 (1994).
18. D. Lytle and B. W. Webb, Air jet impingement heat transfer at low nozzle-plate spacings, *Int. J. Heat Mass Transfer* **37,** 1687–1697 (1994).
19. C. O. Popiel and L. Boguslawaki, Mass or heat transfer in impinging single, round jets emitted by a bell-shaped nozzle and sharp-ended orifice, *Proceedings of the Eighth International Heat Transfer Conference*, pp. 1187–1192 (1986).
20. J. Stevens, Y. Pan and B. W. Webb, Effect of nozzle configuration on transport in the stagnation zone of axisymmetric, impinging free-surface liquid jets—I. Turbulent flow structure, *J. Heat Transfer* **114,** 874–879 (1992).
21. Y. Pan, J. Stevens and B. W. Webb, Effect of nozzle configuration on transport in the stagnation zone of axisymmetric, impinging free-surface liquid jets—II. Local heat transfer, *J. Heat Transfer* **114,** 880–886 (1992).
22. D. T. Vader, F. P. Incropera and R. Viskanta, Local convective heat transfer from a heated surface to an impinging planar jet of water, *Int. J. Heat Mass Transfer* **34,** 611–623 (1991).
23. D. H. Wolf, R. Viskanta and F. P. Incropera, Local convective heat transfer from a heated surface to a planar jet of water with a nonuniform velocity profile, *J. Heat Transfer* **112,** 899–905 (1990).
24. N. T. Obot, A. S. Majumdar and W. J. M. Douglas, The effect of nozzle geometry on impingement heat transfer under a round turbulent jet, ASME Winter Annual Meeting, New York, Paper no. 79-WA/HT-53 (1979).
25. J. Stevens and B. W. Webb, Local heat transfer coefficients under an axisymmetric, single-phase liquid jet, *J. Heat Transfer* **113,** 71–78 (1991).
26. Y. Pan and B. W. Webb, Heat transfer characteristics of arrays of free-surface liquid jets, *General Papers in Heat and Mass Transfer, Insulation and Turbomachinery*, ASME HTD-271, pp. 23–28 (1994).
27. M. T. Scholtz and O. Trass, Mass transfer in a nonuniform impinging jet, *A.I.Ch.E.J.* **16,** 82–96 (1970).
28. E. M. Sparrow and L. Lee, Analysis of flow field and impingement heat/mass transfer due to a nonuniform slot jet, *J. Heat Transfer* **97,** 191–197 (1975).
29. R. A. Rice and S. V. Garimella, Heat transfer from discrete heat sources using an axisymmetric, submerged and confined liquid jet, *Heat Transfer '94, Proceedings of the* 1994 *International Heat Transfer Conference*, Vol. 3, pp. 89–94 (1994).
30. K. Kataoka, M. Suguro, G. Degawa, K. Maruo and I. Mihata, The effect of surface renewal due to large-scale eddies on jet impingement heat transfer, *Int. J. Heat Mass Transfer* **30,** 559–567 (1987).
31. M. D. McGuinness, Flow with a separation bubble: steady and unsteady aspects, Ph.D. Dissertation, Cambridge University Engineering Department (1978).
32. E. P. Sutton, G. P. Evans, M. D. McGuinness and K. M. Svehla, Influence of wall vibrations on a flow with boundary-layer separation at a convex edge, *Unsteady Turbulent Shear Flows*, IUTAM Symposium, Toulouse (Edited by E. Michel *et al.*) 5–8 May, pp. 284–293 (1981).
33. J. A. Fitzgerald, Fluid flow through an axisymmetric jet nozzle, Independent Study Report, Mechanical Engineering Department, University of Wisconsin-Milwaukee (1994).
34. A. J. Ward-Smith, *Pressure Losses in Ducted Flows*, Chapter 4. Butterworths, London (1971).
35. S. Faggiani and W. Grassi, Round liquid jet impingement heat transfer in the region with non-zero pressure gradient, *Eurotherm Seminar No.* 9, Bochum, pp. 105–112 (1989).
36. C. F. Ma and A. E. Bergles, Convective heat transfer on a small vertical surface in an impinging circular liquid jet, *Proceedings of the Second International Symposium of Heat Transfer*, Canton, pp. 248–255 (1988).